JOURNAL OF COMPUTATIONAL PHYSICS 16, 1–19 (1974)

Multifluid Flow Calculations at All Mach Numbers*

FRANCIS H. HARLOW AND ANTHONY A. AMSDEN

University of California, Los Alamos Scientific Laboratory, Los Alamos, New Mexico 87544

Received February 19, 1974

A new fluid dynamics computing technique is described for the solution of time-varying multifluid flows in several space dimensions. An implicit treatment of mass transport, equation of state, and work terms allows for the simultaneous presence of all flow-speed regimes, from far subsonic (incompressible) to far supersonic. Marker particles are used only to follow material interface motions, and are not required through the rest of the computing region. A multiphase process for each calculation cycle combines both Lagrangian and Eulerian viewpoints, and also allows for the convenience of a separate diffusion and dissipation phase, which may be artificial or real, and explicit or implicit. The technique is referred to as the GILA method.

INTRODUCTION

The numerical solution of fluid flow problems involving the time-varying interactions of several materials has usually been accomplished by means of Lagrangian techniques [1]. For one-dimensional problems the Lagrangian approach remains the most efficient and effective for the majority of purposes. The calculation of two- and three-dimensional problems, however, introduces the possibility for strong distortions of the interfaces between materials. The consequence for Lagrangian calculations is loss of accuracy and sometimes even degeneracy to nonsense.

An Eulerian coordinate system for such problems, on the other hand [2], is excellent for the investigation of distortions but lacks the ability to accurately follow material interfaces or to resolve translating fine structure.

Accordingly, there have been developed a variety of hybrid techniques. These include basically Eulerian methods with superimposed interface lines [3] or marker particles [4] for distinguishing between materials, and basically Lagrangian methods with the capability for partial Eulerian rezoning [5]. In this paper, we combine features of several of these hybrid methods, utilizing both the rezoned Lagrangian coordinate mesh and a marker particle system for interface delineation.

* This work was performed under the auspices of the United States Atomic Energy Commission.

Another type of recent development has been the simultaneous implicit treatment of the equation-of-state formula and the mass transport equation [6], which allows for a full range of Mach numbers from zero (the "incompressible" limit) to somewhat greater than unity (the supersonic regime). In the present paper, we extend this implicitness to include the treatment of the work terms in the internal energy equation [7] and the continuity of pressure across an interface. In addition, we extend the multiphase cycle decomposition of the YAQUI technique [5], to include a separate phase for the diffusion and dissipation calculations, and recast the ICE technique [6] into a Lagrangian form utilizing volume as the principal variable, rather than density. Previous arbitrariness in the treatment of internal energy variations in a several-material computational cell is easily resolved by the new features introduced here. The resulting technique here is referred to as the GILA method.

As with most other techniques for the numerical solution of complicated fluid flow problems, the actual calculations can be accomplished only by means of high-speed computers. The following descriptions are therefore written in a manner that is directly related to the necessary computer programs, and illustrated by proof-test examples taken directly from the results of some computer calculations.

Phases of a Calculation Cycle

Subject to prescribed boundary conditions, the calculation develops the solution from prescribed initial conditions through a series of time steps, or cycles. Available data at the beginning of each cycle consist of the initial condtions, or the results of calculations from the previous cycle. From this configuration, the calculations that constitute a full cycle of solution advancement must generate a new configuration that accurately represents the changes occurring during this brief interval of time.

The fluid configuration itself is described in terms of a mesh of cells covering the domain of interest. For each cell there are quantities that vary through time, denoting such variables as average density, pressure, and velocity components. In addition, sets of marker particles are used to show the positions of the interfaces between materials.

These calculations for each cycle in the GILA method can be described in terms of a sequence of three phases. This multiphase split is ideal for isolating specific areas requiring special treatment, for example, very low Reynolds number flows and other circumstances in which additional implicit features are desirable. These three phases are outlined as follows.

Phase I. This is purely Lagrangian, in that the interface marker particles and the mesh of computational cells are assumed to have moved with the fluid during

this phase. In practice, neither the cell vertices nor the marker particles are actually moved in Phase I, this process being deferred to Phase II. Phase I accomplishes the crucial implicit parts of the calculation; the convection, diffusion and dissipation in the other phases can usually be purely explicit for most purposes.

Phase II. The mesh of cells is rezoned, perhaps back to its original location, or else to some other specified configuration. Convective fluxes of mass, momentum, and energy are calculated to account for the difference between actual fluid displacement and net mesh displacement. By calculating only net mesh displacement, the cell vertices need only be moved once per cycle. The convective flux calculations are partly continuous and partly discrete, the distinction being based on the motion of the interface markers.

Phase III. Diffusion and dissipation are calculated. These include both the real effects of viscosity and heat conduction as well as any possible artificially diffusive terms that must be added to counteract the presence of truncation-error terms.

To illustrate the GILA methodology, it is sufficient to describe the special case of a rectangular mesh of cells in plane coordinates, rezoned each cycle back to its original configuration. All of the essential features are thereby demonstrated without the obscuring details that are necessary for the more general case of arbitrary rezone. Our recommended form for the additional rezone complications is essentially that of the YAQUI technique [5].

A simplifying option, appropriate for calculations in which the interface distortions are slight, would treat the interfaces in pure Lagrangian fashion, with the rezone feature being restricted to regions away from the interfaces. This would eliminate the need for marker particles and partially discrete convective fluxes. The present discussion, however, does not make this simplification, since it would eliminate the essential features that we require for general large-distortion studies, which previously have eluded accurate calculation, especially for low Mach number flows along one or more of the coordinate-axis directions.

PHASE I

The starting point for the calculations of this implicit, purely-Lagrangian phase is the equations for conservation of volume and momentum, and a nonconservative form for the internal energy equation,

$$(dV/dt) = \oint \mathbf{n} \cdot \mathbf{u}\, ds, \tag{1}$$

$$M(d\mathbf{u}/dt) = -\oint \mathbf{n}p\, ds + M\mathbf{g}, \tag{2}$$

$$M(dI/dt) = -p(dV/dt). \tag{3}$$

The integration extends over a region of space, moving with the fluid, with fixed mass, M, and varying volume, V. The unit vector, $\mathbf{n}$, is an outward normal; $\mathbf{u}$ is the fluid velocity; p is the pressure; I is the specific internal energy; and $\mathbf{g}$ is the gravitational acceleration.

In place of Eq. (3), we could have used a conservative form for the energy equation, but there are several advantages to the present form, which are offset to an apparently negligible extent by the slight nonconservation of energy observed in our test calculations. One advantage is the considerably easier incorporation of the work terms into the implicit formulation. A second, more important advantage, is the accuracy afforded for high Mach number flows. In fully conservative formulations, slight fluctuations of velocity can be reflected in large fluctuations of temperature, whereas the more direct relationship between work terms and heat variations eliminates this source of temperature inaccuracy.

For the finite-difference version of these equations, we utilize the mesh layout shown in Fig. 1. The velocities and pressure shown there are assumed to be

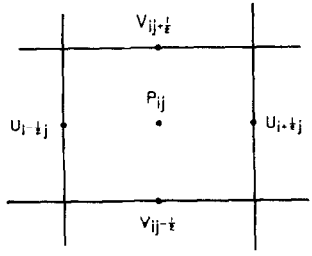

FIG. 1. Velocity and pressure locations in the finite-difference GILA mesh.

continuous across any material interface that may intersect the cell. The implication, as in the PIC method [4], for example, is that both the normal and tangential velocity components are continuous. A much more complicated technique could be developed to remove the restrictions on tangential velocity continuity, but experience has shown that many problems of interest, not previously amenable to numerical solution, can be solved with considerable accuracy even with the present restriction.

Allowing that a material interface may pass through a cell, we require two values for such quantities as mass, volume and specific internal energy, and utilize left subscripts 1 and 2 to denote the two values of each for the cell. In addition, we employ an overbar to designate the new value of a quantity resulting from this phase. In these terms, Eqs. (1)–(3) become

$$(1/\delta t)({}_1\bar{V}_{ij} + {}_2\bar{V}_{ij} - {}_1V_{ij} - {}_2V_{ij}) = (\bar{u}_{i+\frac{1}{2}j} - \bar{u}_{i-\frac{1}{2}j})\,\delta y + (\bar{v}_{ij+\frac{1}{2}} - \bar{v}_{ij-\frac{1}{2}})\,\delta x, \tag{4}$$

$$(M_{i+\frac{1}{2}j}/\delta t)(\bar{u}_{i+\frac{1}{2}j} - u_{i+\frac{1}{2}j}) = (\bar{p}_{ij} - \bar{p}_{i+1j})\,\delta y, \tag{5}$$

$$(M_{ij+\frac{1}{2}}/\delta t)(\bar{v}_{ij+\frac{1}{2}} - v_{ij+\frac{1}{2}}) = (\bar{p}_{ij} - \bar{p}_{ij+1})\,\delta x + M_{ij+\frac{1}{2}} g, \tag{6}$$

$$_1M_{ij}(_1\bar{I}_{ij} - {}_1I_{ij}) = -\bar{p}_{ij}(_1\overline{V}_{ij} - {}_1V_{ij}), \tag{7}$$

$$_2M_{ij}(_2\bar{I}_{ij} - {}_2I_{ij}) = -\bar{p}_{ij}(_2\overline{V}_{ij} - {}_2V_{ij}), \tag{8}$$

while the equations of state and pressure continuity relations become

$$\bar{p}_{ij} = f_1(_1M_{ij}/{}_1\overline{V}_{ij}\,,\ \ {}_1\bar{I}_{ij}), \tag{9}$$

$$\bar{p}_{ij} = f_2(_2M_{ij}/{}_2\overline{V}_{ij}\,,\ \ {}_2\bar{I}_{ij}), \tag{10}$$

in which f_1 and f_2 are prescribed functions of density and specific internal energy. The cell-edge masses, $M_{i+\frac{1}{2}j}$ and $M_{ij+\frac{1}{2}}$, are averages of adjacent total masses. The acceleration of gravity is taken to be g, which is positive upwards and negative downwards.

For efficiency of solution when the fluid is nearly incompressible, it is useful to replace $\bar{p}_{ij}$ by $(r_j + \bar{p}_{ij})$, in which r_j represents the mean hydrostatic equilibrium pressure, given by

$$\frac{r_j - r_{j+1}}{\delta y} = \frac{\langle M_{ij+\frac{1}{2}} \rangle}{\delta x\,\delta y}\, g.$$

The meaning of $\langle\ \rangle$ is an average across the row, the result being a function of j only. With this, the right side of Eq. (5) remains unchanged, while in Eq. (6) it becomes

$$(\bar{p}_{ij} - \bar{p}_{ij+1})\,\delta x + (M_{ij+\frac{1}{2}} - \langle M_{ij+\frac{1}{2}} \rangle)\, g.$$

Thus, for incompressible flows, $\bar{p}$ does not include the mean hydrostatic pressure, while for compressible flows we retain the regular form of Eq. (6).

Thus, there are altogether seven unknown quantities: $_1\overline{V}_{ij}$, $_2\overline{V}_{ij}$, $\bar{p}_{ij}$, $_1\bar{I}_{ij}$, $_2\bar{I}_{ij}$, $\bar{u}_{i+\frac{1}{2}j}$ and $\bar{v}_{ij+\frac{1}{2}}$, for which the seven equations are adequate.

To solve this system by iteration, we use the Chorin–Hirt method [8], which eliminates the requirement for derived boundary conditions (e.g., for pressure gradients at walls), enhances computer efficiency, and relates the convergence criterion to a physically meaningful statement of volume conservation.

To derive the iteration procedure for the present circumstances, we first use Eqs. (4) and (5) to eliminate the unknown velocities from Eq. (4):

$$\begin{aligned}(1/\delta t)(_1\overline{V}_{ij} + {}_2\overline{V}_{ij} - {}_1V_{ij} - {}_2V_{ij}) = {} & (u_{i+\frac{1}{2}j} - u_{i-\frac{1}{2}j})\,\delta y + (v_{ij+\frac{1}{2}} - v_{ij-\frac{1}{2}})\,\delta x \\ & + \delta y^2\,\delta t\left(\frac{\bar{p}_{ij} - \bar{p}_{i+1j}}{M_{i+\frac{1}{2}j}} - \frac{\bar{p}_{i-1j} - \bar{p}_{ij}}{M_{i-\frac{1}{2}j}}\right) \\ & + \delta x^2\,\delta t\left(\frac{\bar{p}_{ij} - \bar{p}_{ij+1}}{M_{ij+\frac{1}{2}}} - \frac{\bar{p}_{ij-1} - \bar{p}_{ij}}{M_{ij-\frac{1}{2}}}\right).\end{aligned} \tag{11}$$

Let $\tilde{p}_{ij}$ be the hth iteration for $\bar{p}_{ij}$, and $(\tilde{p}_{ij} + \delta p_{ij})$ be the $(h + 1)$ st iteration for $\bar{p}_{ij}$. Correspondingly, we let

$$\tilde{u}_{i+\frac{1}{2}j} = u_{i+\frac{1}{2}j} + (\delta y \delta t / M_{i+\frac{1}{2}j})(\tilde{p}_{ij} - \tilde{p}_{i+1j}), \tag{12}$$

$$\tilde{v}_{ij+\frac{1}{2}} = v_{ij+\frac{1}{2}} + (\delta x \delta t / M_{ij+\frac{1}{2}})(\tilde{p}_{ij} - \tilde{p}_{ij+1}) + G_{ij+\frac{1}{2}}, \tag{13}$$

in which

$$G_{ij+\frac{1}{2}} \equiv g\, \delta t$$

for most cases, or, as discussed previously,

$$G_{ij+\frac{1}{2}} \equiv g\, \delta t(1 - [\langle M_{ij+\frac{1}{2}} \rangle / M_{ij+\frac{1}{2}}])$$

for incompressible flows, as a technique to enhance solution efficiency. (For a generalization, this modification could be incorporated automatically, with a discrimination based on Mach number.) As $h \to \infty$, the tilde quantities will converge to the final values for Phase I of the cycle. For the first pressure iteration in Eqs. (12) and (13) one uses the converged pressures derived in the previous cycle, or in the first cycle the prescribed initial pressures. This enables the first iteration for the velocities to be calculated, from which the subsequent changes are calculated by means of the following modified forms of Eqs. (12) and (13):

$$\delta u_{i+\frac{1}{2}j} = (\delta y \delta t / M_{i+\frac{1}{2}j})(\delta p_{ij} - \delta p_{i+1j}), \tag{14}$$

$$\delta v_{ij+\frac{1}{2}} = (\delta x \delta t / M_{ij+\frac{1}{2}})(\delta p_{ij} - \delta p_{ij+1}). \tag{15}$$

In sweeping through the mesh, it is convenient to accumulate the contribution to each of the four surrounding velocity points immediately after the calculation of δp in a cell.

To calculate δp, we are at liberty to choose the iteration level for each of the unknown quantities in Eq. (11) at either h or $h + 1$. For the quantities in cell ij, the choice is $h + 1$; for the surrounding cells, it is h. In preparation for the metamorphosis of Eq. (11) we note that

$$\delta_1 V_{ij} = -\,({}_1V_{ij}^2 / {}_1M_{ij}\, {}_1c_{ij}^2)\, \delta p_{ij}, \tag{16}$$

$$\delta_2 V_{ij} = -\,({}_2V_{ij}^2 / {}_2M_{ij}\, {}_2c_{ij}^2)\, \delta p_{ij}, \tag{17}$$

in which δV again means the change from hth to $(h + 1)$st iteration, and c^2 is the adiabatic sound speed, a known function for each material of the specific internal energy and possibly the density. Also, it is convenient to define

$$\tilde{D}_{ij} \equiv -\frac{{}_1\tilde{V}_{ij} + {}_2\tilde{V}_{ij} - {}_1V_{ij} - {}_2V_{ij}}{\delta x\, \delta y\, \delta t} + \frac{\tilde{u}_{i+\frac{1}{2}j} - \tilde{u}_{i-\frac{1}{2}j}}{\delta x} + \frac{\tilde{v}_{ij+\frac{1}{2}} - \tilde{v}_{ij-\frac{1}{2}}}{\delta y}. \tag{18}$$

Note that when convergence is attained, Eq. (4) implies the vanishing of $\tilde{D}_{ij}$ for every computational cell. Thus, testing for convergence on the basis of sufficiently small $\tilde{D}_{ij}$ gives a physically meaningful interpretation to the criterion employed for terminating the iteration process.

With these substitutions, Eq. (11) becomes

$$\delta p_{ij} = -\tilde{D}_{ij}\, \delta x\, \delta y / H_{ij}\,, \tag{19}$$

in which

$$H_{ij} = \frac{1}{\delta t}\left(\frac{{}_1V_{ij}^2}{{}_1M_{ij}\,{}_1c_{ij}^2} + \frac{{}_2V_{ij}^2}{{}_2M_{ij}\,{}_2c_{ij}^2}\right) + \delta t\left[\delta y^2\left(\frac{1}{M_{i+\frac{1}{2}j}} + \frac{1}{M_{i-\frac{1}{2}j}}\right) + \delta x^2\left(\frac{1}{M_{ij+\frac{1}{2}}} + \frac{1}{M_{ij-\frac{1}{2}}}\right)\right] \tag{20}$$

does not vary through the sequence of iterations.

Thus, in summary, Phase I commences with an initialization of tilde quantities at the values obtained in the previous cycle or, in the case of velocities, calculated by means of Eqs. (12) and (13), and proceeds through an iterative sequence, each iteration containing the following steps.

1. $\tilde{D}_{ij}$ is calculated with Eq. (18),
2. δp_{ij} is calculated with Eq. (19) and the values of $\tilde{p}_{ij}$ are updated,
3. Velocity changes are calculated with Eqs. (14) and (15) and the tilde velocities are updated,
4. Updated values of the volumes and specific internal energies are calculated by means of the simultaneous solution of Eqs. (7)–(10), in which all overbar quantities are replaced by tilde quantities. In the special case of nearly incompressible flow, for example, using an equation of state $p = a^2(\rho - \rho_0)$ with a^2 very large compared to the square of the fluid speed, the convergence rate can be increased considerably by accreting volumes with Eqs. (16) and (17), and by normalizing the sum of the volumes to the required total for the calculation region.

These four steps are repeated until $\tilde{D}_{ij}$ is everywhere small in comparison with a specified convergence criterion.

For simple equations of state (e.g., a polytropic gas) the algebraic solution in the fourth step is easily accomplished. For more complicated equations of state, a numerical procedure (e.g., Newton's method) may be required. Note that updating the volumes is not to be accomplished by means of Eqs. (16) and (17), except in the case of nearly incompressible flow.

The equations described above refer specifically to computational cells containing two different materials. For one-material cells, in which ${}_1M$ or ${}_2M$ is zero, the

equations reduce to the correct form by setting both the mass and volume of the absent material equal to zero (the corresponding value of V^2/Mc^2 also vanishing, for example, in H_{ij}).

By the end of Phase I, implicitly calculated changes have been accomplished for the pressures, velocities, specific internal energies and volumes, subject to the constraint of pressure continuity across the material interface.

Phase II

This phase commences with a mesh displacement from the (not calculated) cell configuration resulting from Phase I to the final rezoned configuration for this cycle. For the present discussion we assume that the mesh is returned to its original layout of rectangular cells. For this or any partial rezoning, the resulting convection must be accomplished and this is the purpose of Phase II. Only for a completely Lagrangian calculation can the convective phase be omitted, but for this and any partial (not purely Eulerian) rezone procedure, the geometrical factors necessary for arbitrary cell shape are much more complicated in the formulations in all three phases [5].

One procedure for calculating the rezone and convective-flux phase would require the use of complicated techniques for sensing the presence of an interface, as described by a line of marker particles or line segments through each cell. One would use this knowledge to discriminate among all the various special cases of orientation and cell–edge intersection in the flux calculations [3].

A simpler approach, however, is to use a cloud of marker particles on both sides of the interface, extending some appropriate distance into each kind of fluid, but not necessarily filling the entire computing region. The motion of these relative to the computing mesh indicates, on a proportional basis, the appropriate flux coefficients to use in the convective transport of mass, momentum, energy, and material kind. Unlike the PIC-method particles [4], these do not really carry convective quantities in proportion to individually stored particle masses, but are used simply to distinguish the *relative* amounts of the various materials convected [9]. It is this second approach that we follow in the present discussion. It should be emphasized that the essence of our technique lies in the procedures of Phase I, and that any other appropriate method for rezone and convection can be used in Phase II, without altering the substance of the implicit phase.

For convenience in this purely Eulerian rezone discussion, we adopt the viewpoint that the cells have not been displaced at all, and that the fluid moves relative to the cells in Phase II. On each side of the interface there is a cloud of marker particles, assumed to extend into the interior of each fluid by a distance of at least one cell dimension. The movement of the particles is accomplished by

interpolating among the adjacent cell velocities to find an effective velocity for each particle in the usual fashion [10]. The technique, which weights each cell velocity in proportion to the overlap area of a particle-centered cell, ensures that particles will not cross over each other, provided that $u_m \delta t/\delta x < 1.0$ and $v_m \delta t/\delta y < 1.0$, in which u_m and v_m are the largest magnitudes of the two velocity components.

For calculating convective fluxes of momentum, we always use a continuous flux procedure. For mass and energy, it must be decided for every cell boundary whether the flux treatment is to be continuous or discrete. Away from any interface, we use a continuous flux calculation, in which the amount of a quantity to be convected is given by the product of its density, the time increment, and the fluxing area. For the density of mass, momentum, or energy, one may use a simple average (corresponding to centered differencing), a donor-cell value (corresponding to "upwind" differencing), or any variably weighted combination of the two. Especially for strongly supersonic flows, the donor-cell differencing for internal energy flux may be required in order to avoid negative values. The details are the same as in many previous techniques.

Discrete fluxing occurs for mass and energy whenever fluid moves from a mixed-fluid cell to a pure-fluid cell, from a mixed-fluid cell to another mixed-fluid cell, and from a pure-fluid cell of one kind to a pure-fluid cell of another kind. The amount of a quantity convected by the discrete-flux calculation depends on the number of marker particles crossing the interface between the two cells. The total amount of mass and energy for each material in the donor cell is equally divided among the current total number of particles of each kind, and this amount is subtracted from the donor cell and added to the receiving cell for every particle crossing the boundary. Only to this extent do the particles themselves enter directly into the calculations; in contrast to the PIC-method particles [4], the present markers carry different amounts every time they cross a cell boundary, depending upon the circumstances at the instant of crossing.

While the conceptual description of discrete fluxing is easily given, the corresponding computer logic is somewhat complicated, especially since the combination with continuous fluxing must be accomplished with strict local conservation throughout the mesh of cells. The full details are omitted from the present discussion.

After the flux calculations have been completed, the new volumes of the two components in each mixed cell must be calculated. For this purpose, we again impose the condition that the equation of state pressures for the two materials

the initial volume of the cell, is sufficient for the purpose. We have observed, incidentally, that for very stiff equations of state, the simultaneous solution for the two volumes can lead to nonsense unless the product of normal density with sound speed is nearly the same for both materials.

It is apparent that discrete fluxing results in step-wise variations, with fineness that depends on the density of marker particles. In one computational cycle there may be no convective flux at all, followed the next cycle by enough to make up for the deficit. Thus, as in PIC-method calculations, there is a certain statistical nature to the results. In many respects, however, the present marker particle approach improves upon the PIC variety.

1. Discrete fluxing occurs only near interfaces, not throughout the region.
2. Discrete mass flux is calculated on the basis of the changing local densities, rather than from the assignment of a fixed mass to each particle.
3. Particle spacing can be much finer, since markers are required only in the vicinity of an interface.
4. Only mass and internal energy are discretely fluxed, the momentum flux being everywhere continuous.

All of these features, combined with the implicit treatment of Phase I, extend considerably the scope of applications for which this new method can be utilized.

PHASE III

Isolation of the calculations in Phase III from the rest has several advantages. For problems with large viscosity or coefficient of heat conduction, it is easier to build in an implicit treatment for enhancing numerical stability. For versatility, the isolation allows the investigator to switch quickly from one type of diffusion to another, among, for example, artificial viscosity, true molecular viscosity, and the turbulent diffusion of mass, momentum and energy [11]. In this phase, too, would be the place to locate the useful anti-truncation-error terms that Rivard and associates [12] have recently found to be especially useful in enhancing accuracy.

In all, there are four parts in Phase III.

1. The artificial diffusion of mass, restricted to diffusion *within* a material kind, but not *between* materials,
2. Momentum diffusion, by artificial viscosity or physical stresses, the latter representing either true viscosity (through coefficients λ and μ, possibly variable) or turbulence (through a Reynolds stress tensor or the simplification afforded by a variable eddy viscosity),
3. Energy diffusion, from molecular or turbulent heat conduction,
4. Dissipation heating, to account for the loss of mean-flow kinetic energy resulting from momentum diffusion.

The equations appropriate for these processes can be exhibited most concisely for the special case of constant diffusion coefficients, the more general cases being direct extensions as appropriate.

The diffusion of mass never takes place between two different materials. In addition, we allow no mass diffusion into or out of a two-material cell, because our experience has shown that if one or both of the mixed-cell materials has an exceptionally stiff equation of state, then even a small amount of mass diffusion can profoundly disturb the continuity-of-pressure condition in the mixed cell.

Between two pure cells of the same material kind, we write

$$\overline{M}_{ij} = M_{ij} + \frac{\tau\,\delta y\,\delta t}{\delta x}\left[\left(\frac{M}{V}\right)_{i+1j} + \left(\frac{M}{V}\right)_{i-1j} - 2\left(\frac{M}{V}\right)_{ij}\right] + \frac{\tau\,\delta x\,\delta t}{\delta y}\left[\left(\frac{M}{V}\right)_{ij+1} + \left(\frac{M}{V}\right)_{ij-1} - 2\left(\frac{M}{V}\right)_{ij}\right] \tag{21}$$

where, as before, an overbar means the new value of a quantity for this phase, and the absence of the overbar means the value at the beginning of this phase. Although V is the same for every cell at this stage of the calculation ($V_{ij} \equiv \delta x \delta y$), we write Eq. (21) as shown to emphasize that mass diffusion flux must be proportional to difference in *density* in the general case.

Momentum diffusion consists of the combined effects of longitudinal (compressive) transport and transverse (shear) transport. The former is especially of importance for the numerical calculation of shocks; the latter may be required for the numerical stability of incompressible flows. Both are required (in more general form than shown below) for truly viscous or turbulent flows. The appropriate form can be illustrated as follows.

$$\begin{aligned}\bar{u}_{i+\frac{1}{2}j}\overline{M}_{i+\frac{1}{2}j} = u_{i+\frac{1}{2}j}M_{i+\frac{1}{2}j} + \frac{\delta t}{\delta x}\Big[&M_{i+1j}Q_{i+1j}\,(u_{i+\frac{3}{2}j} - u_{i+\frac{1}{2}j}) \\ &- M_{ij}Q_{ij}(u_{i+\frac{1}{2}j} - u_{i-\frac{1}{2}j})\Big] + \frac{A\,\delta t}{\delta y}\,[M_{i+\frac{1}{2}j+\frac{1}{2}}(u_{i+\frac{1}{2}j+1} - u_{i+\frac{1}{2}j}) \\ &- M_{i+\frac{1}{2}j-\frac{1}{2}}(u_{i+\frac{1}{2}j} - u_{i+\frac{1}{2}j-1})],\end{aligned} \tag{22}$$

$$\begin{aligned}\bar{v}_{ij+\frac{1}{2}}\overline{M}_{ij+\frac{1}{2}} = v_{ij+\frac{1}{2}}M_{ij+\frac{1}{2}} + \frac{\delta t}{\delta y}\,&[M_{ij+1}Q_{ij+1}(v_{ij+\frac{3}{2}} - v_{ij+\frac{1}{2}}) \\ &- M_{ij}Q_{ij}(v_{ij+\frac{1}{2}} - v_{ij-\frac{1}{2}})] + \frac{A\,\delta t}{\delta x}\,[M_{i+\frac{1}{2}j+\frac{1}{2}}(v_{i+1j+\frac{1}{2}} - v_{ij+\frac{1}{2}}) \\ &- M_{i-\frac{1}{2}j+\frac{1}{2}}(v_{ij+\frac{1}{2}} - v_{i-1j+\frac{1}{2}})].\end{aligned} \tag{23}$$

Q_{ij} is a variable coefficient, which, for artificial viscosity, would be a positive constant for a compressive region and zero (or possibly a negative constant to alleviate truncation-error effects) in an expansive region. In this simple form, A is a constant with the dimensions of velocity.

For internal energy, we proceed in two stages. The first is the heat conduction part

$$\begin{aligned}\overline{M}_{ij}I'_{ij} = M_{ij}I_{ij} &+ (B\,\delta y\,\delta t/\delta x)(I_{i+1j} + I_{i-1j} - 2I_{ij}) \\ &+ (B\,\delta x\,\delta t/\delta y)(I_{ij+1} + I_{ij-1} - 2I_{ij})\end{aligned} \tag{24}$$

in which B is a positive constant.

Finally, the dissipation of kinetic energy in Phase III is calculated. The process of momentum diffusion alters the kinetic energy in two ways, a redistribution and a net decrease. The former should have no effect on internal energy, while account for the latter must be reflected in an increase in internal energy. To describe this dissipation, we calculate

$$\begin{aligned}\delta I_{ij} = Q_{ij}\Big[&\frac{\delta t}{\delta x}(u_{i+\frac{1}{2}j} - u_{i-\frac{1}{2}j})^2 + \frac{\delta t}{\delta y}(v_{ij+\frac{1}{2}} - v_{ij-\frac{1}{2}})^2\Big] \\ &+ \frac{A\,\delta t}{16}\Big[\frac{1}{\delta y}(u_{i+\frac{1}{2}j+1} + u_{i-\frac{1}{2}j+1} - u_{i+\frac{1}{2}j-1} - u_{i-\frac{1}{2}j-1})^2 \\ &+ \frac{1}{\delta x}(v_{i+1j+\frac{1}{2}} + v_{i+1j-\frac{1}{2}} - v_{i-1j+\frac{1}{2}} - v_{i-1j-\frac{1}{2}})^2\Big]\,.\end{aligned} \tag{25}$$

For a pure (unmixed) cell,

$$\bar{I}_{ij} = I'_{ij} + \delta I_{ij}\,.$$

For a two-material cell, we simultaneously solve

$${}_1\overline{M}_{ij}({}_1\bar{I}_{ij} - {}_1I'_{ij}) + {}_2\overline{M}_{ij}({}_2\bar{I}_{ij} - {}_2I'_{ij}) = ({}_1\overline{M}_{ij} + {}_2\overline{M}_{ij})\,\delta I_{ij} \tag{26}$$

and the continuity equation for pressure,

$$f_1({}_1\overline{M}_{ij}/{}_1\overline{V}_{ij}\,,\,{}_1\bar{I}_{ij}) = f_2({}_2\overline{M}_{ij}/{}_2\overline{V}_{ij}\,,\,{}_2\bar{I}_{ij}).$$

This dissipation calculation is not rigorously conservative of energy, but experience with a variety of calculations shows that the discrepancy is not appreciable. We have tried an alternative procedure in which the change of kinetic energy in each cell is locally balanced by a corresponding change in internal energy. While this is rigorously conservative, the results are poor, because this reflects both the dissipation *and* the rearrangement of kinetic energy into the internal energy profile, rather than just the net dissipation.

Discussion

The essential features of the GILA method have been described in the preceding paragraphs. They form the basis for numerous possible extensions, some of which have already been mentioned. Others that have been considered are discussed briefly in this section.

For calculations in cylindrical coordinates with an azimuthal velocity, the extensions are straightforward. The incorporation of a centrifugal term is easily accomplished in Phase I, during the initialization of the tilde velocities. With axial symmetry, the azimuthal velocity remains unchanged in Phase I, the convective and coriolis terms being calculated in Phase II, with the viscous stress effects added in Phase III. This version, currently being developed for the study of tornados and dust devils, will be reported later [13].

A special case to be considered has one material at a very much smaller density than the other. Air–water interactions are an interesting example. At the extreme, one of the materials could even be required to represent a vacuum. In the case of such a mismatch in density, it is expected that the equation of state for the heavier material would have the qualitative features of a "stiffened gas " [14], for which we write

$$p = a^2(\rho - \rho_0) + (\gamma - 1)\,\rho I. \tag{27}$$

If the coefficient a^2, sufficiently exceeds the level of internal energy, I, then the pressure can vanish for a density that does not differ appreciably from the "normal" density, ρ_0. Thus the "mixed" cell iteration (with material and vacuum) can satisfactorily converge to the correct free-surface vanishing of normal stress. Note, however, that for low-Reynolds-number flows, the viscous contribution to the normal-stress condition may be appreciable, in which case its presence is required in Phase I for both freesurface and multimaterial calculations. In a very large but finite density mismatch, a near equilibrium in pressure may result in subsonic flow on one side and supersonic flow on the other, in which case the implicit features of Phase I are of especially great importance.

Some Sample Calculations

To demonstrate the validity of the GILA method, we have performed a variety of calculations, both one-dimensional and two-dimensional. The one-dimensional studies were of two types, uniform translation of an interface and the shock tube.

The uniform translation studies were designed to show that the interface treatment would allow a pair of materials initially in uniform equilibrium to propagate at constant velocity through the computational mesh without appreciable departures from uniformity. The results, of course, show that absolute uniformity cannot be maintained, except under very special conditions, the departures depending principally on the density of marker particles. We first examined a slightly supersonic flow. With a sparse cloud on each side of the interface (eight rows of particles on each side), the fluctuations of fluid velocity nearby averaged about 5%; with a finer spacing (twenty five rows on each side) the fluctuations were reduced to about

1 %. The same calculations for far subsonic translation were performed with very large specific internal energy, and alternatively with a^2 very large in Eq. (27), with resulting fluctuations distinctly smaller than those for the supersonic test.

The principal goals of the shock tube calculations were to examine the consequences of the new implicit features, and to see if the interface treatment allows for calculations [15]. The results for a two-to-one density ratio are shown in Fig. 2,

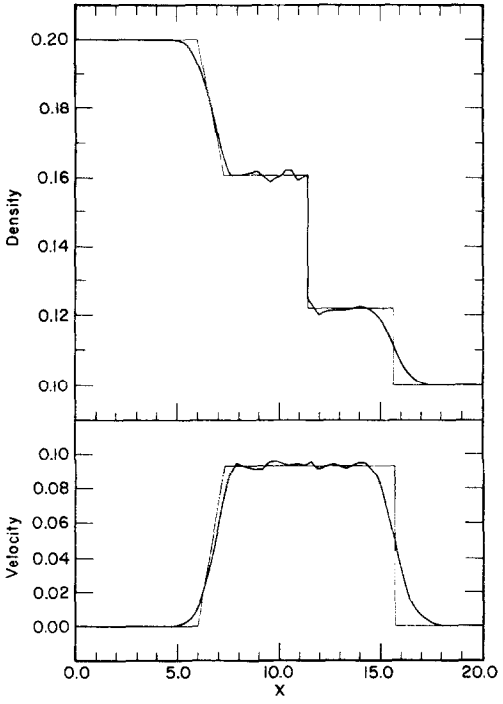

FIG. 2. One-dimensional GILA calculation of a 2:1 density-ratio shock tube.

which demonstrates the well-resolved contact surface. At the same time, the shock and rarefaction regions are also well-represented, in comparison with the analytical solutions shown in the figure.

In the two-dimensional examples, the interface was allowed to distort considerably. We illustrate the accuracy of results by comparison with the calculations of Daly [16] for the Rayleigh–Taylor instability of two superimposed fluids with a density ratio of 2 : 1. His completely incompressible calculations were simulated in the GILA-program run by choosing 0.01 as the Mach number for the initial perturbation. Figures 3 and 4 show that the results are nearly identical.

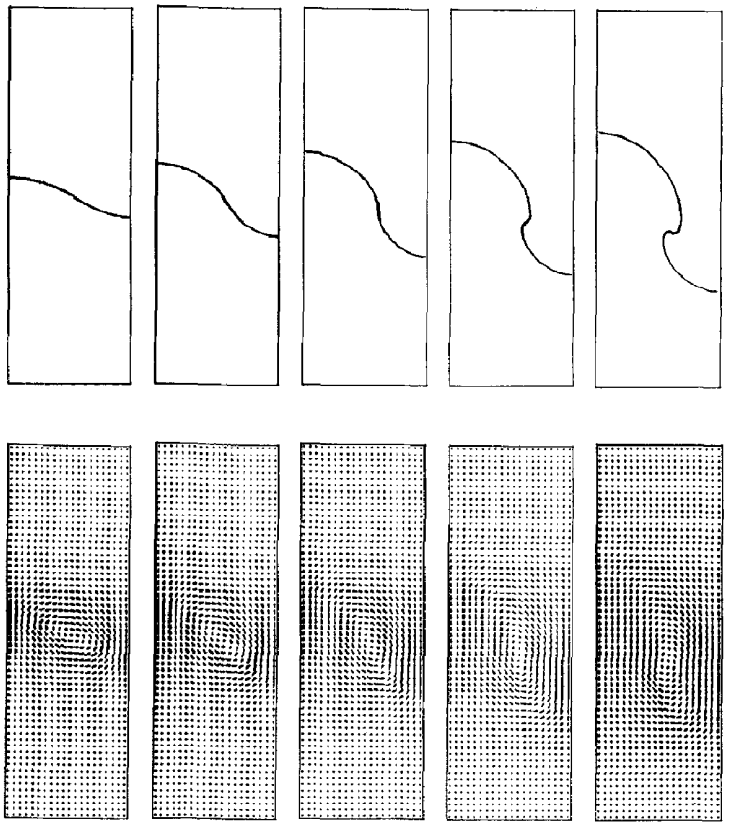

FIG. 3. Two-fluid GILA calculation of incompressible Rayleigh–Taylor interface instability with a 2:1 density ratio. The upper sequence shows the interface position and the lower sequence shows the velocity vectors, at problem times 0.045, 0.089, 0.134, 0.179, and 0.218.

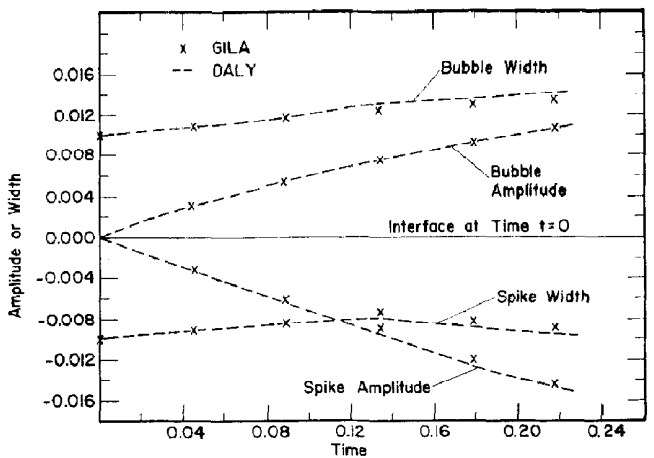

FIG. 4. A comparison of the spike and bubble amplitudes and widths from the calculation in Fig. 3 with those calculated by Daly.

The next step in our study was to examine the results at other Mach numbers. Figure 5 contrasts the behavior for the small and large Mach number cases. For incompressible flow, the initial consequence of a sheet perturbation applied to the interface is the development of flow with vanishing divergence extending well into both fluids. With a perturbation at near unit Mach number, the very different appearance comes about through the development of compression and rarefaction regions.

In a slight variation of the problem, we applied the same perturbation to an interface with no density discontinuity, and watched the subsequent oscillatory

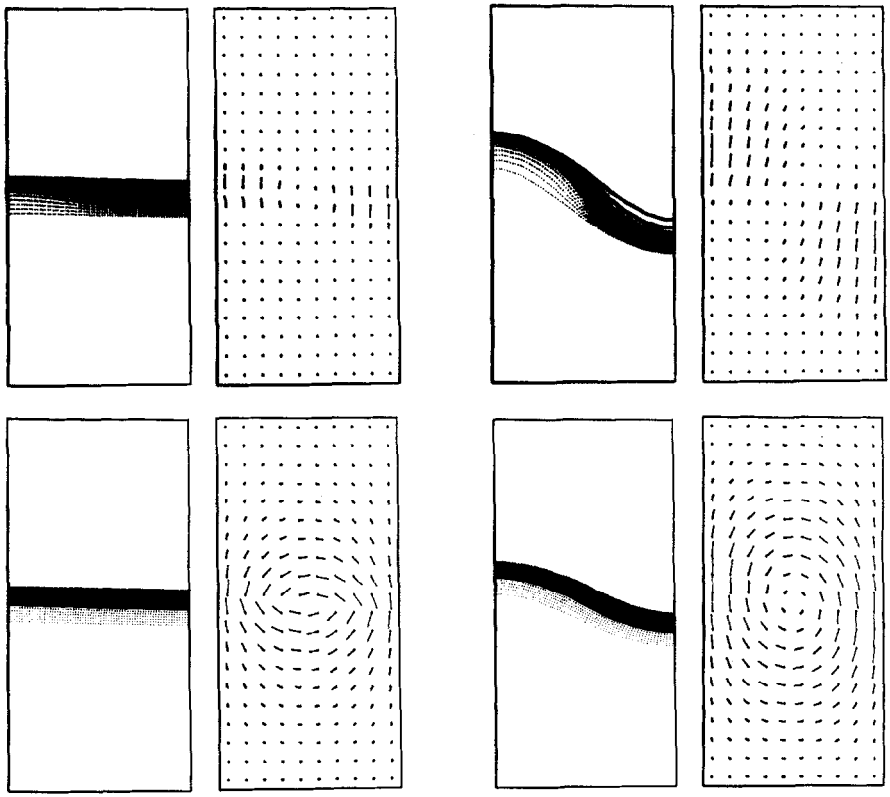

FIG. 5. Early stages of two interface instability calculations, contrasting the behavior for large and small Mach number cases. The plots are paired sequences of particles and velocity vectors. Lengths of vectors plotted are scaled to the instantaneous maximum velocity in the mesh. In the upper set, calculated with $a^2 = 0$, the effects of compressibility are evident. Problem times shown are 0.08 and 1.60, and the maximum velocities at these two times are 0.54 and 0.12. The lower set is from the same times in a calculation with $a^2 = 10^4$, well in the incompressible regime. Maximum velocities are reduced to 0.15 and 0.07.

coasting. Commencing from a unit-Mach-number perturbation, the initial stages consisted of the propagation of shocks and sound signals throughout the confined region of the box. The explicit incorporation of viscosity damped the motion to the extent that linear theory was applicable for the development of a comparison solution. A normal-mode analysis showed various possible frequencies for the motion, the computer calculation of which is illustrated by velocity vector plots in Fig. 6. Each of the modes decreases in amplitude with its own decay rate. A logarithmic plot of the maximum fluid speed in the system shows that the predicted frequencies can be identified and the decay-rate slopes confirmed. Our experience indicates that no explicit procedure exists that can perform this type of far-subsonic

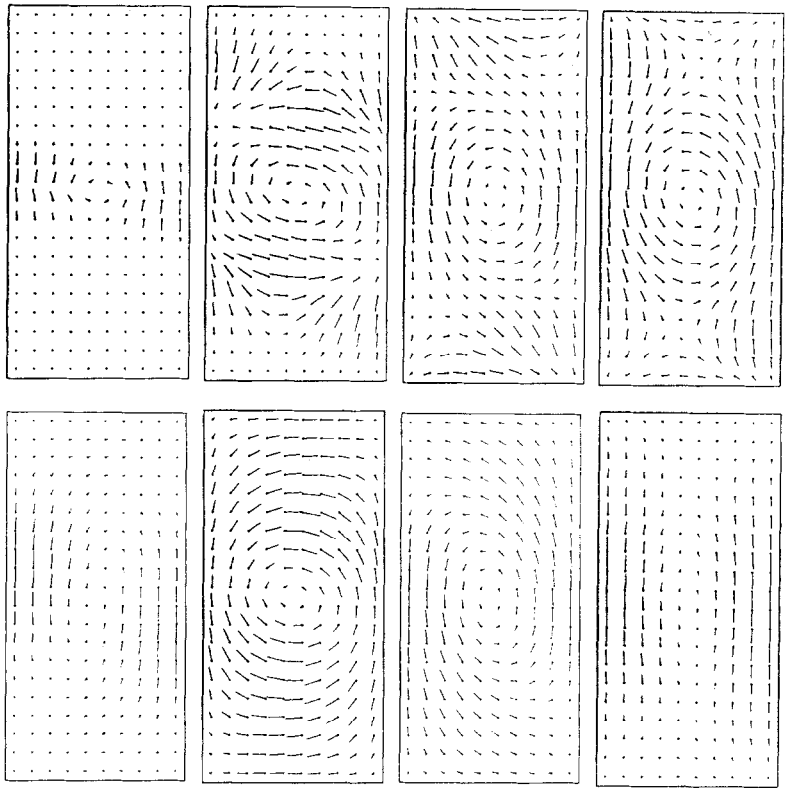

FIG. 6. A calculation similar to the upper sequence in Fig. 5 ($a^2 = 0$), but with no density discontinuity across the perturbed interface. The resulting oscillatory coasting is shown by velocity vectors at problem times 0.10, 0.60, 1.10, 1.60, 2.10, 2.60, 3.10, and 3.60, reading across, then down. Maximum velocities are damping slowly through viscous effects, and are in the 0.04 range in the last three frames.

calculation, in which the effects of compressibility are crucial to the development of an oscillatory mode.

The conclusions from these and other studies performed with our proof-test code are that the GILA technique extends considerably the capability to calculate complicated fluid flow problems, with several materials distorting strongly at either low or high Mach number, in a multidimensional domain. The efficiency and convenience of the multiphase procedure was apparent throughout the developments. Various alternatives were explored for each of the phases, and our experience shows that even further optimization is possible, especially in the calculation of convective fluxes in Phase II, for which greater accuracy may eventually be achieved by means of completely continuous fluxing rather than the partially discrete version described for the present work.

REFERENCES

1. See, for example, F. H. HARLOW, "Numerical Methods for Fluid Dynamics, An Annotated Bibliography," Los Alamos Scientific Laboratory Report LA-4281, 1969; F. H. HARLOW, (Ed.), "Computer Fluid Dynamics—Recent Advances," AIAA Selected Reprint Series, Volume XV, New York, 1973.
2. R. A. GENTRY, R. E. MARTIN AND B. J. DALY, An Eulerian differencing method for unsteady compressible flow problems, *J. Comp. Phys.* **1** (1966), 87.
3. M. RICH, "A method for Eulerian fluid dynamics," Los Alamos Scientific Laboratory Report LAMS-2826, 1963.
4. F. H. HARLOW, The particle-in-cell method for numerical solution of problems in fluid dynamics, *Proc. Symp. Appl. Math.* **15**, 269, 1963; see also Ref. [1].
5. A. A. AMSDEN AND C. W. HIRT, "YAQUI: An arbitrary Lagrangian–Eulerian computer program for fluid flow at all speeds," Los Alamos Scientific Laboratory Report LA-5100, 1973.
6. F. H. HARLOW AND A. A. AMSDEN, A numerical fluid dynamics calculation method for all flow speeds, *J. Comp. Phys.* **8** (1971), 197.
7. Independent suggestions from J. Young and B. Thompson.
8. C. W. HIRT AND J. L. COOK, Calculating three-dimensional flows around structures and over rough terrain, *J. Comp. Phys.* **10** (1972), 324.
9. J. D. KERSHNER AND C. L. MADER, "2DE: A two-dimensional continuous Eulerian hydrodynamic code for computing multicomponent reactive hydrodynamic problems," Los Alamos Scientific Laboratory Report LA-4846, 1972.
10. A. A. AMSDEN AND F. H. HARLOW, "The SMAC method: A numerical technique for calculating incompressible fluid flows," Los Alamos Scientific Laboratory Report LA-4370, 1970.
11. F. H. HARLOW, Ed., "Turbulence Transport Modeling," AIAA Selected Reprint Series, Volume XIV, New York, 1973.
12. W. C. RIVARD, T. D. BUTLER AND O. A. FARMER, "A method for increased accuracy in Eulerian fluid dynamics calculations," Los Alamos Scientific Laboratory Report LA-5426-MS, 1973.
13. L. R. STEIN, personal communication.
14. F. H. HARLOW AND A. A. AMSDEN, "Fluid dynamics," Los Alamos Scientific Laboratory Monograph LA-4700, 1971.

15. C. W. HIRT, Heuristic stability theory for finite-difference equations, *J. Comp. Phys.* **2** (1968), 339.
16. B. J. DALY, A numerical study of two-fluid Rayleigh–Taylor instability, *Phys. Fluids* **10** (1967), 297.